Nanoscale

Cite this: *Nanoscale*, 2011, **3**, 2481

www.rsc.org/nanoscale

COMMUNICATION

In situ monitoring of single molecule binding reactions with time-lapse atomic force microscopy on functionalized DNA origami†

Na Wu,[a] Xingfei Zhou,[b] Daniel M. Czajkowsky,[a] Ming Ye,[a] Dongdong Zeng,[a] Yanming Fu,[a] Chunhai Fan,[a] Jun Hu[a] and Bin Li*[a]

Received 17th February 2011, Accepted 25th March 2011
DOI: 10.1039/c1nr10181a

Individual biomolecular binding events were recorded *in situ* by combining time-lapse atomic force microscopy and DNA origami. Single streptavidin molecules bound to specifically biotinyated DNA origami were simply counted as a function of time to obtain a direct measure of the binding rate.

The interactions between biomolecules play an essential role in effecting their functions within living organisms. A variety of methods is available to study biomolecules at the single-molecule level in real time, which offers an opportunity to obtain information that might otherwise be obscured by ensemble averaging.[1–4] Of the single-molecule methods, atomic force microscopy (AFM) has proven to be a powerful tool for investigating the behavior of biomolecules owing to its nanoscale spatial resolution in a liquid environment.[5–8] One key factor limiting the resolution in this methodology is the flat substrate that supports and immobilizes the objects to be imaged. Mica is a widely used substrate in AFM due to its atomic flatness over large areas.[9–12] However, for the case of imaging in a liquid, it is critical that the biomolecule be firmly fixed to the surface; otherwise, the object will be pushed along by the tip. APTES, divalent cations, and other molecules have been used to modify mica to enhance adsorption of DNA and protein–DNA complexes for imaging molecular topography.[13–15] In the case of recording reaction processes with AFM, a more rigorous strategy for attaching the molecules should been carried out. There are successful cases for studying protein–DNA and protein–protein reactions already.[16–22] Recently, with the assistance of lipid bilayers and streptavidin (SA) crystals as functional surfaces, a high-speed AFM greatly broadened the usefulness of AFM for biological research. Several dynamic biomolecular processes have been recorded directly, providing insight at the single-molecule level.[23,24] In the search for a new platform to enable deeper investigation into the behavior of single molecules, the particular strategy of attachment must be sufficiently robust to endure both the periodical tip scanning and the liquid exchange, when some of the reactants are added. In addition, other factors such as the biomolecule's activity, orientation, and configuration when attached to the surface must be taken into account. More importantly, how to distinguish between the specific and the non-specific interactions of the single biomolecules in a multiple component system, a long standing problem in AFM techniques, should be overcome, since the identification of objects in AFM images mostly depends on their limited topography information.

Here, we develop a system that combines high spatial resolution of AFMs with nanoscale multifunctional origami as a surface for supporting and fixing biomolecules to study single-molecule reactions. DNA origami is constructed by folding a long single-strand DNA sequence (usually M13mp18 viral DNA) with the help of hundreds of short oligonucleotide staple strands.[25] So far, many DNA origami scaffolds, 2D-, and 3D-architectures, have been designed and constructed.[26–31] Moreover, a great deal of materials such as nanoparticles, biomolecules and viruses have been combined to decorate the origami into beautiful and functional configurations.[32–37] Very recently, the plastic and addressable features of origami have been exploited in several single-molecule studies. Some examples of detecting single molecule reactions and single molecular behavior such as the binding and breaking of chemical bonds, single-molecule kinetics, molecular robot movement, the response of singlet oxygen to a single photosensitizer, and the hTopo18-DNA cleavage complexes bound with its bait DNA were demonstrated by using origami nanostructures as templates.[38–42] Since the studied molecules can be localized to specific positions on the origami surface with nanometre resolution, the specific and the nonspecific binding events can be easily distinguished by AFM imaging. Although DNA origami has been used as a functionalized surface for single-molecule study by AFM, monitoring biochemical reactions in real time *in situ* has not been heretofore described.

In this paper, DNA origami was used as a functionalized surface for monitoring the streptavidin–biotin binding reaction *in situ* by time-lapse AFM. The streptavidin–biotin system is widely used for biomolecule labeling, purification, immobilization and patterning and it is also a prototypical reaction system in studies of protein–protein, protein and peptide reactions.[43,44] Streptavidin (SA) is a tetramer, and each subunit can bind biotin with high affinity and selectivity.[45] The DNA origami, programmed into a rectangle shape, shows a flat shape and can be easily biotinylated with designed numbers and at defined sites. Because biotin is a small molecule, it is

[a]*Laboratory of Physical Biology, Shanghai Institute of Applied Physics, Chinese Academy of Sciences, Shanghai, 201800, China. E-mail: libin@sinap.ac.cn; Fax: +86-21-59552394; Tel: +86-21-39194603*
[b]*Physical Department, Ningbo University, Ningbo Zhejiang, China*
† Electronic supplementary information (ESI) available: AFM images of DNA origami before and after exposure to 200 nM thrombin for 30 min. See DOI: 10.1039/c1nr10181a

essentially undetectable in the AFM images, and therefore, only the topography of the origami, a flat area of hundreds of nanometres, is observed. SA, with a molecular weight of 65 kD, is clearly visible as protrusions in AFM images of origami surfaces.[46] Thus, the binding events could be easily detected based on the topography changes of the DNA origami surface by AFM (Fig. 1).

To prepare a biotinylated origami, a rectangular-shaped DNA origami was constructed according to a modified version of the preparation described in ref. 47 and 48 and several oligonucleotide staple strands were replaced by biotinylated oligonucleotide staple strands at the correspondence sites. Briefly, M13mp18 viral DNA (New England Biolabs, Inc. catalogue number: # 4040S) and over 200 short oligonucleotide staple strands (Sangon Biotech Co., Ltd, Shanghai, P. R. China) were mixed with 1 × TAE buffer (Tris, 40 mM; acetic acid, 20 mM; EDTA, 2 mM; magnesium chloride, 12.5 mM; pH 8.0) in a molar ratio of 1 : 10 with a total volume of 100 μl, then the mixture was put in an Eppendorf Mastercycler Personal machine to enable annealing from 95 °C to 20 °C at a rate of 0.1 °C every 10 s for ~ 2 h. In this particular case, there are four biotin sites located on each origami (Fig. 1), providing four sites for streptavidin–biotin binding reactions. This design also enables identification of the two orientations, either facing up or facing down, if it is immobilized randomly on the mica surface.

For the AFM experiments (at room temperature), a drop of 5 μl of the biotinylated origami solution was deposited on freshly cleaved mica for 2 min, and then the sample was mounted on a J scanner of the AFM (Multi-mode Nanoscope IIIa, Vecco/Digital Instruments, Santa Barbara, CA). To get a clear image and maintain a lower loading force on the scanning objects, the AFM parameters, such as gain, setpoint, and scanning speed were carefully adjusted. Imaging was performed in tapping mode, with a typical scan speed of 2 Hz, using a 0.58 N m^{-1} tip (NPS, Veeco, CA). At such a scan speed, one image was acquired within 3 min, setting the lower limit of the time resolution in the present experiment. To study the binding events of a single streptavidin–biotin reaction, a particular concentration of SA (Sangon Biotech Co., Ltd, Shanghai, P. R. China) was slowly injected into the liquid cell of the AFM after first obtaining an image of the biotinylated origami sample. The tip was continuously scanning during the experiment to enable real-time monitoring of the complete binding reaction.

We found that the surface topography of the sample surface indeed changed as a function of time. As illustrated in Fig. 2, before injection, the surface of mica and the origami are smooth, both in large or small scanning regions (Fig. 2a). The average length, width and height of the origami are 102.5 ± 3.3 nm, 71.1 ± 1.8 nm and 2.4 ± 0.1 nm, (n = 240) respectively, agreeing well with design parameters. After SA injection (to a final concentration 7.6 nM), some spots appear on the surface of the DNA origami and the spot numbers increase steadily over time (Fig. 2b–f). The average height of these spots is 3.4 ± 0.5 nm (as shown in Fig. 2g and h), which is similar to the height observed of 2D SA crystals on biotinylated bilayers.[49] The spots were observed only at the expected locations, based on the design parameters for the biotinylated oligonucleotide strands, so we believe the spots are the SA molecules. Consistent with this interpretation, when we increased the SA concentration to 76 nM, the spots appeared immediately after the injection, and occupied all of the biotinylated accessible sites on the origami, with no other spots at

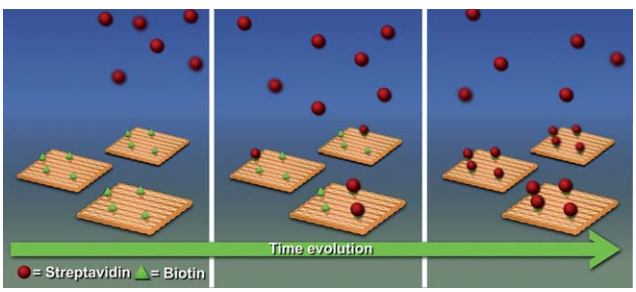

Fig. 1 Probing of the streptavidin–biotin binding reaction on DNA origami *in situ* at the single molecule level. The biotinylated sites on the origami are marked by triangles, and the DNA origami and SA are represented by rectangles and dots, respectively.

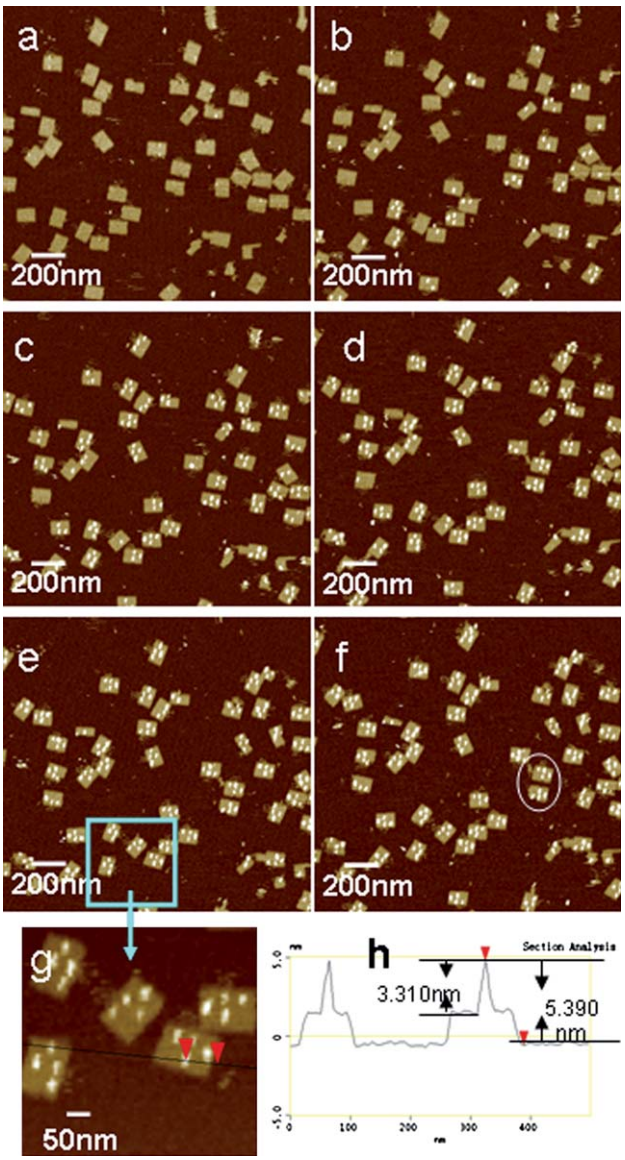

Fig. 2 A series of AFM images of the biotin–streptavidin binding processes. (a) Before SA injection. (b)–(f) After SA injection, at 2.5 min, 7.5 min, 10.0 min, 20 min and 25 min, respectively. (g) An enlarged feature from the area of (e) shown by the rectangle. (h) Section scheme of the black line in (g). The height scale for all images is 7 nm.

other places such as the mica or the other regions of the origami. These results indicate that the binding specificity is excellent, with very little nonspecific adsorption, leading to a low noise for the imaging system. Such a high level of specificity, to some degree, overcomes the significant obstacle of identifying the features within the topographic image, which is generally one of the AFM limitations for heterogeneous system study. To further confirm the potential of the origami scaffold as able to monitor highly specific reactions with biomolecules, thrombin was introduced into the system to a final concentration of 200 nM, yet, no spots appear on origami surface, even after 30 min (see supporting information†).

As reported in earlier studies, labeling methods (radioactive isotope, fluorescence dye), and surface plasmon resonance (SPR) measurements have been used to study the (avidin)streptavidin–biotin binding activities.[50–54] Here, the biotinylated origami, a functional surface for site binding reactions, provides the advantages of low nonspecific adsorption and high reaction specificity, which makes it possible to observe binding spots clearly at single-molecule level. By simply counting the binding spots one by one, we can determine the exact binding rate from the scanning area. In Fig. 2a, there are 160 biotinylated sites on the 40 intact DNA origami blocks within the scanning area of 1.8 μm^2. About two minutes after injection of the SA solution, 57 spots appeared on the biotinylated sites, yielding a binding extent of 35.6%. Statistic data ($n = 3$) identifies two types of binding rates within 30 min of imaging (Fig. 3). A fast binding rate is observed at the beginning of SA addition, and lasts for almost 15 min. Then a relative slow binding rate continues for the next 15 min. The SA–biotin reaction approaches nearly 100% at a given SA concentration in our experiments.

To detect the dissociation rate of the SA–biotin bond, the same area was scanned repeatedly for another 30 min, but the bright spots largely remained on the origami scaffold, suggesting that the binding is strong. This observation also indicates that this bond can endure the repeated scanning of the AFM tip, which is very important for the detection of binding events of single biomolecules.

Although repeatedly scanning the same region revealed no disturbance of the SA–biotin complexes, we sought to make sure whether the force applied by tip scanning has any effect on the binding rate detection. To this end, a small area was scanned continuously 5–8 times and then the scan size was increased. The

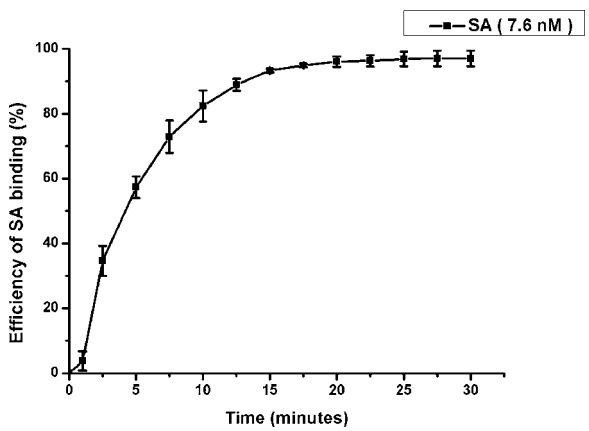

Fig. 3 Streptavidin–biotin binding rate as a function of time. The binding rate is determined by fitting the data of three-group experiments with a concentration of SA 7.6 nM.

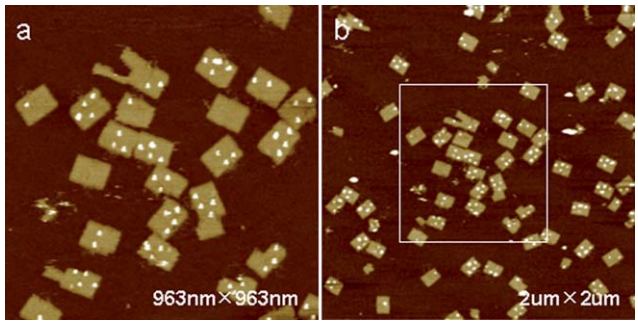

Fig. 4 Comparison of the streptavidin–biotin binding rate between areas (a) and (b). (a) This area was scanned 8 times and showed a degree of binding of 68%. (b) This area was then scanned once and the degree of binding was found to be 72% (not including the area marked by the white frame in which the binding rate is 68%).

images show no obvious difference between these two regions, although statistical analysis of the data indicated perhaps slight differences in the binding extent, usually between 1–3% (maximally, 4%) (Fig. 4). These results suggest that the disturbing activities of the tip may still have some effect on the measured binding rates of biomolecules, though the effect may be small. The tip–sample interaction appeared to lower the rate of apparent binding rate in our case.

A previous report indicated that there are some DNA origami facing down and some facing up on the mica surface.[25,38] Interestingly, we found that the binding reaction could occur even on surfaces when the origami was facing down (Fig. 2f, within the white circle, there are two origamis, one facing down and one facing up). We suggest that the biotin molecule is accessible from either surface. The ability to observe binding to either face of the origami could not be easily found by traditional ensemble averaging method or by single-molecule fluorescence due to a relatively low space resolution. In this case, the detailed information of the binding differences could easily be detected and quantified by just imaging and counting, suggesting a new and simple way for single-molecule reaction study.

In summary, a simple method for time-lapse imaging of single molecule reactions *in situ* was developed by using DNA origami as a reaction surface. The whole dynamic process of the streptavidin–biotin binding reaction was recorded. At a SA concentration of 7.6 nM, the binding ratio increased steadily up to nearly 100% within 30 min. This novel single-molecule reaction detection method, at the nanometre scale, may prove useful to study other macromolecule behavior and reaction kinetics.

Acknowledgements

This work was financially supported by the National Natural Science Foundation (10874198, 21073222, 11074137), the National Basic Research Program of China (2007CB936000), the Ministry of Health (2009ZX10004-301), the Chinese Academy of Sciences (KJCX2-EW-N03), the Chinese Academy of Sciences Fellowships for Young International Scientists (2009YA1-1) and the Shanghai Municipal Commission for Science and Technology (0952nm04600).

References

1 H. P. Lu, L. Y. Xun and X. S. Xie, *Science*, 1998, **282**, 1877–1882.
2 X. W. Zhuang, L. E. Bartley, H. P. Babcock, R. Russell, T. J. Ha, D. Herschlag and S. Chu, *Science*, 2000, **288**, 2048.

3 N. A. Tanner, J. J. Loparo, S. M. Hamdan, S. Jergic, N. E. Dixon and A. M. van Oijen, *Nucleic Acids Res.*, 2009, **37**, e27.
4 P. S. Spuhler, J. Knezevic, A. Yalcin, Q. Bao, E. Pringsheim, P. Droge, U. Rant and M. S. Unlu, *Proc. Natl. Acad. Sci. U. S. A.*, 2010, **107**, 1397–1401.
5 B. Drake, C. B. Prater, A. L. Weisenhorn, S. A. C. Gould, T. R. Albrecht, C. F. Quate, D. S. Cannell, H. G. Hansma and P. K. Hansma, *Science*, 1989, **243**, 1586–1589.
6 C. Bustamante, C. Rivetti and D. J. Keller, *Curr. Opin. Struct. Biol.*, 1997, **7**, 709–716.
7 C. Rivetti, M. Guthold and C. Bustamante, *EMBO J.*, 1999, **18**, 4464–4475.
8 L. S. Shlyakhtenko, V. N. Potaman, R. R. Sinden, A. A. Gall and Y. L. Lyubchenko, *Nucleic Acids Res.*, 2000, **28**, 3472–3477.
9 L. T. Cai, H. Tabata and T. Kawai, *Appl. Phys. Lett.*, 2000, **77**, 3105–3106.
10 P. K. Hansma, J. P. Cleveland, M. Radmacher, D. A. Walters, P. E. Hillner, M. Bezanilla, M. Fritz, D. Vie, H. G. Hansma, C. B. Prater, J. Massie, L. Fukunaga, J. Gurley and V. Elings, *Appl. Phys. Lett.*, 1994, **64**, 1738–1740.
11 F. Ostendorf, C. Schmitz, S. Hirth, A. Kuhnle, J. J. Kolodziej and M. Reichling, *Nanotechnology*, 2008, **19**, 305705.
12 H. Poppa and A. G. Elliot, *Surf. Sci.*, 1971, **24**, 149.
13 J. Hu, M. Wang, H. U. G. Weier, P. Frantz, W. Kolbe, D. F. Ogletree and M. Salmeron, *Langmuir*, 1996, **12**, 1697–1700.
14 H. G. Hansma, D. E. Laney, M. Bezanilla, R. L. Sinsheimer and P. K. Hansma, *Biophys. J.*, 1995, **68**, 1672–1677.
15 H. Mueller, H. J. Butt and E. Bamberg, *J. Phys. Chem. B*, 2000, **104**, 4552–4559.
16 D. Pastre, L. Hamon, I. Sorel, E. Le Cam, P. A. Curmi and O. Pietrement, *Langmuir*, 2010, **26**, 2618–2623.
17 S. Kasas, N. H. Thomson, B. L. Smith, H. G. Hansma, X. S. Zhu, M. Guthold, C. Bustamante, E. T. Kool, M. Kashlev and P. K. Hansma, *Biochemistry*, 1997, **36**, 461–468.
18 I. Sorel, O. Pietrement, L. Hamon, S. Baconnais, E. Le Cam and D. Pastre, *Biochemistry*, 2006, **45**, 14675–14682.
19 Y. K. Jiao, D. I. Cherny, G. Heim, T. M. Jovin and T. E. Schaffer, *J. Mol. Biol.*, 2001, **314**, 233–243.
20 F. Kienberger, H. Mueller, V. Pastushenko and P. Hinterdorfer, *EMBO Rep.*, 2004, **5**, 579–583.
21 S. J. T. van Noort, K. O. van der Werf, A. P. M. Eker, C. Wyman, B. G. de Grooth, N. F. van Hulst and J. Greve, *Biophys. J.*, 1998, **74**, 2840–2849.
22 M. B. Viani, L. I. Pietrasanta, J. B. Thompson, A. Chand, I. C. Gebeshuber, J. H. Kindt, M. Richter, H. G. Hansma and P. K. Hansma, *Nat. Struct. Biol.*, 2000, **7**, 644–647.
23 D. Yamamoto, N. Nagura, S. Omote, M. Taniguchi and T. Ando, *Biophys. J.*, 2009, **97**, 2358–2367.
24 N. Kodera, D. Yamamoto, R. Ishikawa and T. Ando, *Nature*, 2010, **468**, 72.
25 P. W. K. Rothemund, *Nature*, 2006, **440**, 297–302.
26 L. L. Qian, Y. Wang, Z. Zhang, J. Zhao, D. Pan, Y. Zhang, Q. Liu, C. H. Fan, J. Hu and L. He, *Chin. Sci. Bull.*, 2006, **51**, 2973–2976.
27 S. M. Douglas, A. H. Marblestone, S. Teerapittayanon, A. Vazquez, G. M. Church and W. M. Shih, *Nucleic Acids Res.*, 2009, **37**, 5001–5006.
28 Y. G. Ke, S. M. Douglas, M. H. Liu, J. Sharma, A. C. Cheng, A. Leung, Y. Liu, W. M. Shih and H. Yan, *J. Am. Chem. Soc.*, 2009, **131**, 15903–15908.
29 A. Kuzuya and M. Komiyama, *Nanoscale*, 2010, **2**, 310–322.
30 A. Kuzuya and M. Komiyama, *Chem. Commun.*, 2009, 4182–4184.
31 A. M. Hung, C. M. Micheel, L. D. Bozano, L. W. Osterbur, G. M. Wallraff and J. N. Cha, *Nat. Nanotechnol.*, 2010, **5**, 121–126.
32 H. Bui, C. Onodera, C. Kidwell, Y. Tan, E. Graugnard, W. Kuang, J. Lee, W. B. Knowlton, B. Yurke and W. L. Hughes, *Nano Lett.*, 2010, **10**, 3367–3372.
33 B. Sacca, R. Meyer, M. Erkelenz, K. Kiko, A. Arndt, H. Schroeder, K. S. Rabe and C. M. Niemeyer, *Angew. Chem., Int. Ed.*, **49**, 9378–9383.
34 R. Chhabra, J. Sharma, Y. G. Ke, Y. Liu, S. Rinker, S. Lindsay and H. Yan, *J. Am. Chem. Soc.*, 2007, **129**, 10304.
35 A. Kuzuya, M. Kimura, K. Numajiri, N. Koshi, T. Ohnishi, F. Okada and M. Komiyama, *ChemBioChem*, 2009, **10**, 1811–1815.
36 K. Numajiri, M. Kimura, A. Kuzuya and M. Komiyama, *Chem. Commun.*, 2010, **46**, 5127–5129.
37 N. Stephanopoulos, M. H. Liu, G. J. Tong, Z. Li, Y. Liu, H. Yan and M. B. Francis, *Nano Lett.*, 2010, **10**, 2714–2720.
38 N. V. Voigt, T. Torring, A. Rotaru, M. F. Jacobsen, J. B. Ravnsbaek, R. Subramani, W. Mamdouh, J. Kjems, A. Mokhir, F. Besenbacher and K. V. Gothelf, *Nat. Nanotechnol.*, 2010, **5**, 200–203.
39 R. Jungmann, C. Steinhauer, M. Scheible, A. Kuzyk, P. Tinnefeld and F. C. Simmel, *Nano Lett.*, 2010, **10**, 4756–4761.
40 K. Lund, A. J. Manzo, N. Dabby, N. Michelotti, A. Johnson-Buck, J. Nangreave, S. Taylor, R. J. Pei, M. N. Stojanovic, N. G. Walter, E. Winfree and H. Yan, *Nature*, 2010, **465**, 206–210.
41 S. Helmig, A. Rotaru, D. Arian, L. Kovbasyuk, J. Arnbjerg, P. R. Ogilby, J. Kjems, A. Mokhir, F. Besenbacher and K. V. Gothelf, *ACS Nano*, 2010, **4**, 7475–7480.
42 R. Subramani, S. Juul, A. Rotaru, F. F. Andersen, K. V. Gothelf, W. Mamdouh, F. Besenbacher, M. D. Dong and B. R. Knudsen, *ACS Nano*, 2010, **4**, 5969–5977.
43 S. P. Song, Y. Qin, Y. He, Q. Huang, C. H. Fan and H. Y. Chen, *Chem. Soc. Rev.*, 2010, **39**, 4234–4243.
44 M. Howarth, D. J. F. Chinnapen, K. Gerrow, P. C. Dorrestein, M. R. Grandy, N. L. Kelleher, A. El-Husseini and A. Y. Ting, *Nat. Methods*, 2006, **3**, 267–273.
45 N. M. Green, *Methods Enzymol.*, 1990, **184**, 51–67.
46 Z. Zhang, D. D. Zeng, H. W. Ma, G. Y. Feng, J. Hu, L. He, C. Li and C. H. Fan, *Small*, 2010, **6**, 1854–1858.
47 Y. G. Ke, S. Lindsay, Y. Chang, Y. Liu and H. Yan, *Science*, 2008, **319**, 180–183.
48 A. E. Gerdon, S. S. Oh, K. Hsieh, Y. Ke, H. Yan and H. T. Soh, *Small*, 2009, **5**, 1942–1946.
49 I. Reviakine and A. Brisson, *Langmuir*, 2001, **17**, 8293–8299.
50 H. F. Launer and H. Fraenkelconrat, *J. Biol. Chem.*, 1951, **193**, 125–132.
51 Y. Hiller, J. M. Gershoni, E. A. Bayer and M. Wilchek, *Biochem. J.*, 1987, **248**, 167–171.
52 J. R. Wayment and J. M. Harris, *Anal. Chem.*, 2009, **81**, 336–342.
53 L. S. Jung, K. E. Nelson, P. S. Stayton and C. T. Campbell, *Langmuir*, 2000, **16**, 9421–9432.
54 M. Srisa-Art, E. C. Dyson, A. J. Demello and J. B. Edel, *Anal. Chem.*, 2008, **80**, 7063–7067.

